Improved Thermal Shock Resistance of Magnesium Aluminate Spinel Ceramics by Aluminium Titanate Additions

K. Moritz, Chr. G. Aneziris

The capability of aluminium titanate additions to improve the thermal shock resistance of alumina-rich magnesium aluminate spinel refractories was investigated. Raw material mixtures with different maximum particle sizes of 20 µm, 1 mm, or 3 mm were used. The strength and the dynamic Young's modulus of the spinel ceramic at room temperature were decreased by aluminium titanate, whereas the resistance to thermal shock, tested by water quenching from 950 °C, was enhanced. The dynamic Young's modulus of the Al_2TiO_5-containing samples exhibited a pronounced hysteresis as a function of temperature.

1 Introduction

Carbon-free oxide refractories with improved resistance to thermal shock are of great importance for industrial steel casting and other metal casting processes. In contrast to carbon-bonded refractories, harmful emissions, arising from the pyrolysis of resin or coal tar pitch during the manufacturing process of the carbon-bonded materials, can be avoided. The research project, being part of the Priority Program 1418 (Refractory – Initiative to Reduce Emissions – FIRE) of the German Research Foundation, has been focused on the improvement of the refractory properties of sintered oxide ceramics for applications such as nozzles or nozzle inlay parts in steel casting.

High-alumina ceramics from synthetic raw materials are known to show high refractoriness, chemical stability, corrosion resistance, and good wear hardness [1, 2], but the thermal shock properties of pure sintered alumina are poor [3]. For enhancing the thermal shock resistance, the influence of ZrO_2, TiO_2 and/or SiO_2 additions on the microstructure and properties of alumina ceramics was investigated in the first period of this project from 2009 to 2012 [4–7]. A material composition of 95 mass-% Al_2O_3, 2,5 mass-% ZrO_2 and 2,5 mass-% TiO_2 (AZT) led to promising results. In previous investigations, a low Young's modulus and an increased thermal shock resistance compared with pure Al_2O_3 were found for an AZT ceramic of very similar composition and explained by the formation of zones with different thermal expansion coefficients acting as "spring elements" between the Al_2O_3 grains [8]. In the first phase of the present project, an increased bending strength of AZT ceramics (sintered at 1650 °C) after quenching from 1200 °C was measured. Even after the 5th thermal shock from this temperature, the strength was higher than the initial value. This behaviour was mainly attributed to an aluminium titanate (Al_2TiO_5) phase formed during sintering. Further crystalline phases identified by means of X-ray diffraction were srilankite, monoclinic zirconia, rutile, and the main phase corundum [4, 5]. It is known from the literature that typical properties of aluminium titanate – such as low mechanical strength and Young's modulus, low thermal expansion, low thermal conductivity, and the resultant excellent thermal shock resistance of Al_2TiO_5 ceramics – are due to a microcrack structure which is formed during cooling-down from sintering temperature because of a strong anisotropy of thermal expansion along the three crystallographic axes [9–12]. It is also well-known that Al_2TiO_5 is instable in the temperature range from about 900 – 1280 °C and decomposes reversible into Al_2O_3 and TiO_2. The decomposition rate depends on various factors including temperature, holding time, heating rate, atmosphere, phase purity, grain size, and additives [13]. Several oxidic additives, such as MgO [13, 14] or Fe_2O_3 [15], can stabilize the titanate phase. Because of the different theoretical densities of the starting materials and the reaction product, the formation of aluminium titanate (TD = 3,70 g/cm^3) from corundum and rutile (TD = 3,99 and 4,25 g/cm^3, respectively) is accompanied by an increase in volume [16], its decomposition by volume shrinkage. The Al_2TiO_5 phase in the above-mentioned AZT ceramic underwent partial decomposition when it was heated to 1200 °C in the quenching experiments, as shown by means of X-Ray Diffraction (XRD) and Electron Backscatter Diffraction (EBSD) studies. This partial decomposition was assumed to contribute to the observed increase in strength as a result of the thermal shock test [4, 5]. Nozzles made of AZT with a length of 125 mm, an outer diameter of 20 mm, and a wall thickness of 5 mm were tested in a Metal Casting Simulator (MCS). 50 kg of steel

Kirsten Moritz, Christos G. Aneziris
Technische Universität Bergakademie Freiberg,
Institute of Ceramics, Glass and Construction Materials
09596 Freiberg
Germany

Corresponding author: *K. Moritz*
E-mail: Kirsten.Moritz@ikgb.tu-freiberg.de

Keywords: magnesium aluminate spinel, aluminum titanate, thermal shock resistance, dynamic Young's modulus

Received: 10.12.2015
Accepted: 14.01.2016

Tab. 1 Summary of the investigated samples

Maximum Particle Size of the Raw Material	Al_2TiO_5 Content [mass-%]		
	0	12	16
20 µm	x	x	x
1 mm	x	x	–
3 mm	x	x	–

Tab. 2 Raw material mixtures with maximum particle sizes of 1 mm and 3 mm

Kind of Samples → / Raw Material ↓		Content [mass-%]			
		<1 mm, without Al_2TiO_5	<1 mm, 12 mass-% Al_2TiO_5	<3 mm, without Al_2TiO_5	<3 mm, 12 mass-% Al_2TiO_5
AR 78	0–0,02 mm	18	13	24	18
	0–0,045 mm	0	0	0	2
	0–0,09 mm	16	16	12	10
	0–0,2 mm	17	2	12	0
	0–0,5 mm	34	42	26	32
	0,5–1 mm	15	15	11	11
	1–3 mm	0	0	15	15
Al_2TiO_5		0	12	0	12

melt with a temperature of 1620 °C flowed through each of the test nozzles which had been preheated to 1000 °C for avoiding freezing of the molten steel. As shown by means of computed tomography, the MCS test did not lead to a detectable damage of the nozzles [6].

In cooperation with another subproject of the Priority Program 1418, the AZT refractory and a pure alumina ceramic were investigated by wedge splitting tests at Forschungszentrum Jülich/DE. Mechanically weaker boundaries between coarser grains led to lower strength and elastic modulus of the AZT ceramic, but the material exhibited a rising crack resistance with crack extension due to local friction or bridging between crack surfaces and macroscopic crack branching [17]. The thermal shock parameter R"" according to Hasselman [18] predicted, consistent with the above-mentioned quenching tests, a higher thermoshock resistance of the AZT ceramic compared with pure alumina [17].

Based on the positive results of the first project phase, the influence of aluminium titanate on the thermal shock resistance of alumina-rich magnesium aluminate spinel has been investigated in the 2nd period from 2012–2015.

Magnesium Aluminate (MA) spinels are important refractory materials due to a combination of beneficial characteristics such as high strength at elevated temperatures and high corrosion resistance to basic slags. Stoichiometric MA spinel contains 71,8 mass-% Al_2O_3 and 28,2 mass-% MgO, but solid solutions with higher alumina or magnesia contents in a wide range can be formed at high temperatures and maintained by rapid cooling [19]. A material containing approximately 78 mass-% of Al_2O_3 was used in the present work. The spinel phase with this composition remains stable at temperatures around 1600 °C, e.g., during steel production [19].

The authors started their investigations using a MA spinel powder with a particle size <20 µm. Pre-synthesized aluminium titanate or Al_2O_3- and TiO_2-powder were added. According to the 2nd route, Al_2TiO_5 was in situ formed during sintering. Compared with the pure spinel ceramic, both routes led to an improved thermal shock resistance tested by repeated quenching from 950 °C or 1150 °C [20, 21]. In further investigations, presented in the present paper, also materials with coarser grain sizes have been studied.

2 Experimental

For investigating the influence of aluminium titanate additions and the grain size distribution of the raw material on the properties of the magnesium aluminate spinel ceramic, test specimens from seven different mixtures (Tab. 1) were produced by slip casting. The used spinel raw material was the product AR 78 from Almatis/DE. According to manufacturer's data, the magnesia content of this alumina-rich MA spinel material ranges from 20,5 – 24,0 mass-%. The material contains small amounts of impurities: CaO (<0,30 mass-%), SiO_2 (<0,20 mass-%), Na_2O (<0,32 mass-%), Fe_2O_3 (<0,25 mass-%), and magnetic Fe (<0,02 mass-%) [22]. Different grain size fractions of AR 78 are available.

Aluminum titanate was synthesized by reaction sintering of corundum powder Martoxid MR 70 (Albemarle) and rutile powder Tronox TR (Crenox) at 1650 °C with 4 h holding time (for more details see [21]). The reaction product was ground in a planetary mill Pulverisette 5 (Fritsch/DE) using zirconia grinding beakers and balls. By means of the particle size analyser LS 230 (Beckman Coulter), the median particle diameter of the obtained powder was determined to be 4,2 µm.

For fabricating green bodies from coarse-grained raw material with a maximum particle size of 1 mm or 3 mm, the particle size distributions were adjusted on the basis of the particle packing model according to Dinger and Funk [23] (distribution modulus 0,25) by mixing different fractions of AR 78 and, for preparing the samples with aluminium titanate, the pre-synthesized Al_2TiO_5 powder. Some modifications compared to the calculated ideal distributions were necessary based on experience regarding slip casting. Suspensions of the powder mixtures listed in Tab. 2 and suspensions containing only the finest AR 78 grain-size fraction (0–20 µm) with and without Al_2TiO_5 were prepared in an Eirich intensive mixer (Maschinenfabrik Gustav Eirich/DE). The solid content of the suspensions was in the range between 83 – 92 mass-%. Dolapix CE 64 was used as dispersant and Optapix AC 170 as binding agent (both from Zschimmer & Schwarz/DE). Prismatic test specimens (length × width × height = 150 mm × 25 mm × 25 mm) were produced by slip casting into plaster moulds.

The samples were dried at 110 °C. Afterwards, the organic additives were burnt out at 650 °C. Green bodies from the powder with a maximum particle size of 20 µm were sintered in air at a temperature of

1550 °C, those from the raw material with particle sizes <1 mm or <3 mm because of the lower sintering activity of coarser powders at 1650 °C. The dwell time was 2 h in both cases.

The apparent (open) and true (total) porosity of the sintered samples were measured according to DIN E 993-1 by means of the water immersion method using the Archimedes' principle. A helium pycnometer Accupyc 1330 (Micromeritics) was used for measuring the true densities of the sintered materials, required for determining the total porosities, according to DIN 66317 2. The pore size distributions of the sintered bodies were determined by mercury intrusion using a Pascal 440 porosimeter (Thermo Scientific). Micrographs of polished sections were produced by means of a scanning electron microscope XL-30 ESEM FEG (FEI) with Backscatter Electron (BSE) detector.

At least 5 sintered prismatic test specimens of each kind of sample with the above-mentioned dimensions were subjected to thermal shock from 950 °C to room temperature by quenching in water.

In accordance with DIN EN 993-6, the 3-point bending strength of sintered bodies before and after thermal shock was determined using a TIRAtest 2420 testing machine (TIRA/DE). The dynamic Young's modulus at room temperature was measured both by ultrasonic testing and by impulse excitation. Two different ultrasonic measuring systems were used: an Ultrasonic tester BP-700 Pro (UltraTest Dr. Steinkamp & Büssenschütt/DE) and an UKS-D system equipped with transmitter and receiver pair UPG/UPE-D (Geotron Elektronik/DE). By means of the impulse excitation technique using a Resonant Frequency Damping Analyser RFDA HTVP 1600 (IMCE/BE), the Young's modulus was not only measured at room temperature but also as a function of temperature according to following schedule:

- heating at 3 K/min up to 1600 °C,
- 1 h holding time at 1600 °C,
- cooling at 3 K/min up to 600 °C and without a preset rate up to room temperature.

In order to find out whether aluminium titanate is (partially) decomposed during this measurement, the maximum temperature was reduced to 1150 °C and the holding time prolonged to 2 h. This temperature was chosen because, as generally accepted, the highest decomposition rate of aluminium titanate is reached in the range from 1100 – 1150 °C [24], whereas the phase may be regenerated at temperatures above 1300 °C [25[. Further samples were heat-treated in a high-temperature furnace (Nabertherm/DE) according to the same schedule.

The heat-treated samples and as-sintered specimens were comminuted in a vibratory disc mill (Retsch/DE) with tungsten carbide grinding set and investigated by XRD using an X'Pert PRO MPD 3040/60 diffractometer (PANalytical) with CuK_α radiation and the software X'Pert High-Score.

Tab. 3 True and apparent porosities of the sintered samples

Particle Size of the Raw Material/ Sintering temperature	Al_2TiO_5 Content [mass-%]	True Porosity [%]	Apparent Porosity [%]
<20 µm/1550 °C	0	15,4 ± 0,6	14,6 ± 0,3
	12	5,1 ± 0,2	4,2 ± 0,2
	16	5,0 ± 0,2	4,5 ± 0,2
<1 mm/1650 °C	0	21,1 ± 0,4	19,0 ± 0,4
	12	17,6 ± 0,4	15,7 ± 0,3
<3 mm/1650 °C	0	18,9 ± 0,2	17,0 ± 0,1
	12	13,8 ± 0,5	12,2 ± 0,4

3 Results and discussion

One of the important factors influencing the properties of ceramics is the porosity. The true and apparent porosities of the different sintered samples, measured by the water immersion method, are listed in Tab. 3.

Regarding the influence of the grain size distribution of the raw material, samples with and without aluminium titanate showed the same trend. Sintered bodies from the finest grain-size fraction (<20 µm) had the lowest porosities, those from the materials mixtures with particle sizes <1 mm the highest. Although both the <1 mm and the <3 mm mixtures were adjusted on the basis of the particle packing model according to Dinger and Funk (see section 2), a closer particle packing seemed to be achieved in practice for the <3 mm mixtures.

The pore sizes increased in the same order (Fig. 1, Tab. 4). Comparing the apparent porosities determined by water immersion (Tab. 3) and mercury intrusion (Tab. 4) shows that both methods led to similar results. Please note that only one of each kind of samples was investigated by mercury porosimetry, whereas the porosities measured by

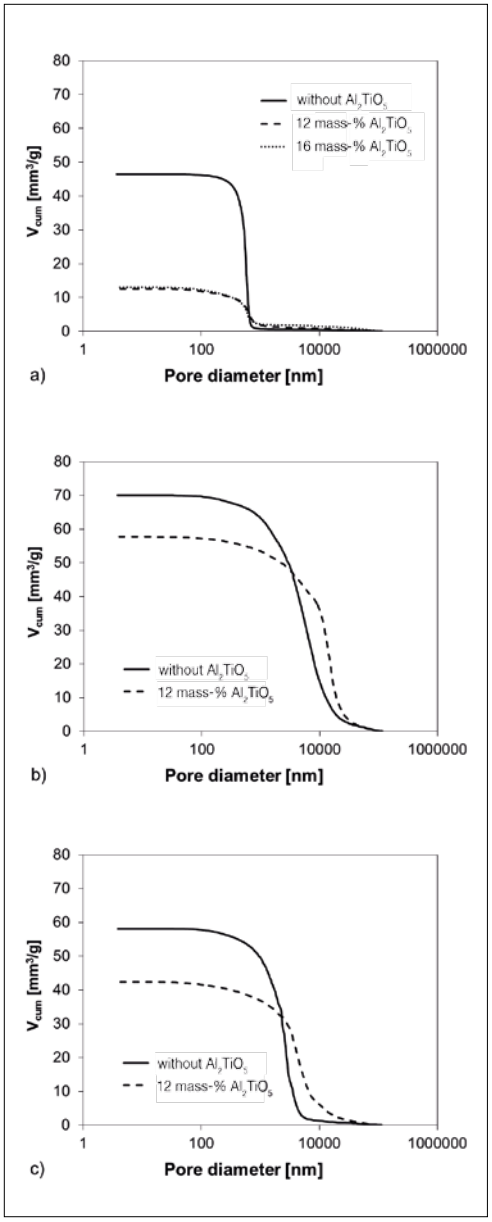

Fig. 1 Cumulative pore volume vs. pore diameter of sintered bodies fabricated from raw materials with different maximum particle size: a) <20 µm, b) <1 mm, c) <3 mm

Tab. 4 Results of mercury intrusion porosimetry

Particle Size of the Raw Material/ Sintering Temperature	Al_2TiO_5 Content [mass-%]	Porosity by Hg Intrusion [%]	Median Pore Diameter [µm]	Modal Pore Diameter [µm]
<20 µm/1550 °C	0	14,2	0,5	0,6
	12	4,4	0,6	0,6
	16	4,4	0,6	0,6
<1 mm/1650 °C	0	19,6	5,1	7,9
	12	17,0	12,5	15,6
<3 mm/1650 °C	0	17,0	2,4	2,9
	12	13,0	4,2	4,4

the water immersion method are average values and thus more significant.

In all cases, the addition of aluminium titanate led to a higher densification of the samples (Tab. 3 – 4) pore size distributions of the coarse-grained samples to higher pore diameters (Fig. 1, Tab. 4). As already reported in our previous publications on MA spinel ceramics from the powder fraction <20 µm [20, 21], samples with Al_2TiO_5 exhibited in comparison with the pure spinel samples significantly enhanced grain growth during sintering. This effect was confirmed in the present work for all kinds of samples. An example can be seen in Fig. 2 showing details of the microstructures of sintered bodies from the raw material mixtures with a maximum grain size of 3 mm. As confirmed by elemental analysis by Energy Dispersive Spectroscopy (EDS), the lighter phase in Fig. 2b is aluminium titanate. The lower porosities and the increased grain growth of the Al_2TiO_5-containing samples can be attributed to the influence of TiO_2. Titania is known to promote sintering of various ceramic materials including alumina and magnesium aluminate spinel [26, 27].

The strength measured by three-point bending tests and the dynamic Young's modulus of the as-sintered samples at room temperature are shown in Fig. 3 and Fig. 5, respectively. Young's modulus measurements using different methods (see section 2) gave similar results. Comparing the investigated samples without aluminium titanate shows that, as expected, the highest strength and Young's modulus were obtained at the lowest porosity (i.e., with the grain size fraction of the raw material <20 µm) and the lowest values at the highest porosity (i.e., with the raw material mixture <1 mm). The mechanical properties of the specimens from the mixtures with

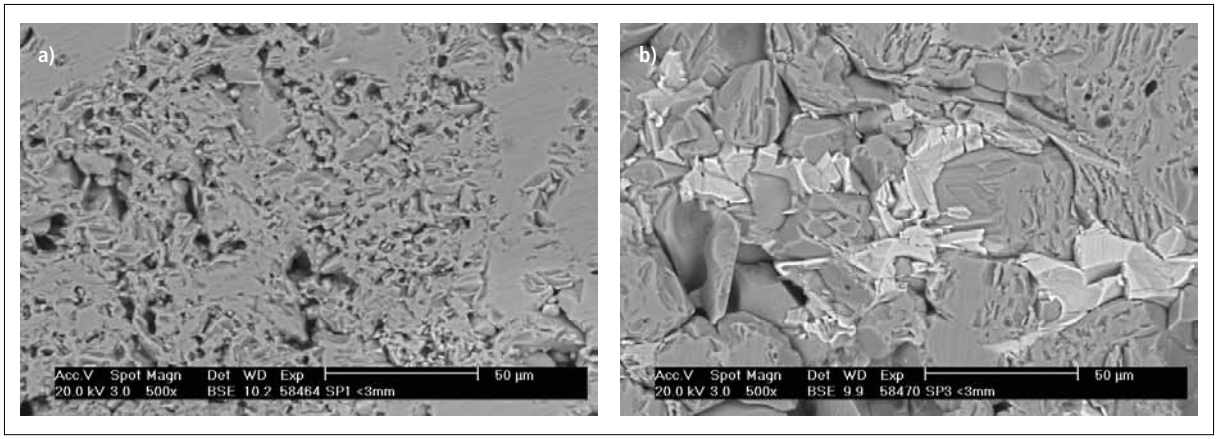

Fig. 2a–b BSE images of sintered samples from AR 78 <3 mm without Al_2TiO_5 (a), and with 12 mass-% Al_2TiO_5 (b)

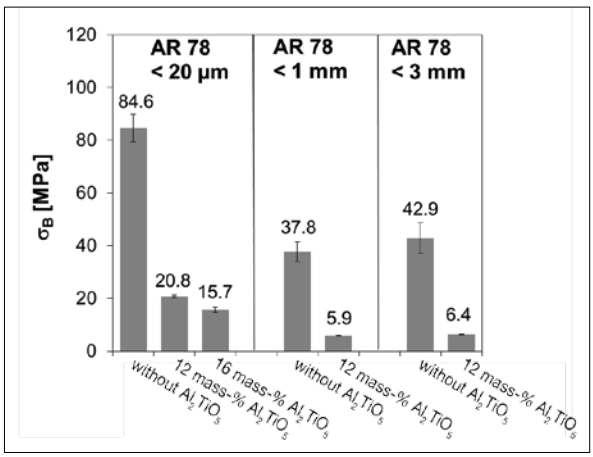

Fig. 3 Three-point bending strength of the sintered bodies

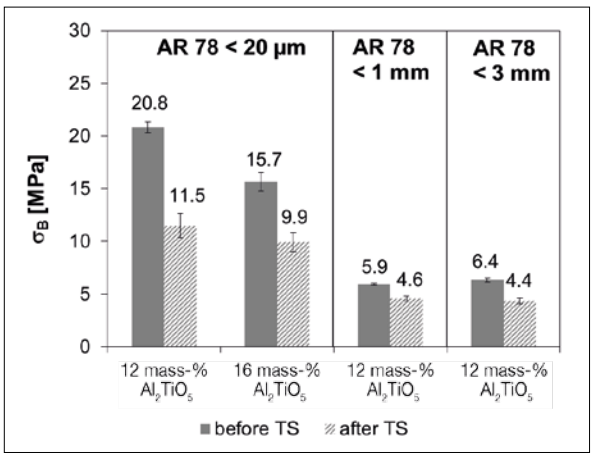

Fig. 4 Three-point bending strength of the Al_2TiO_5-containing sintered bodies before and after quenching from 950 °C

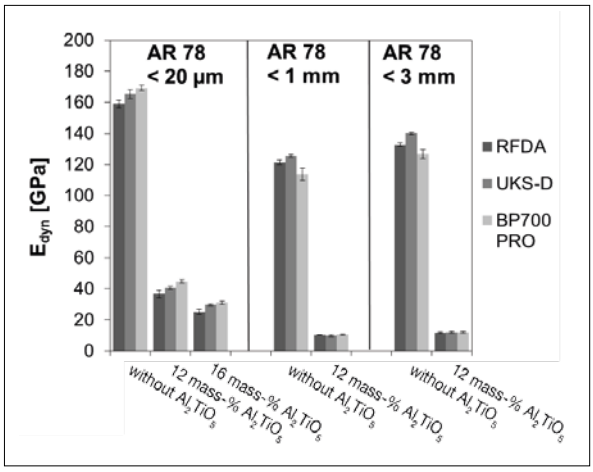

Fig. 5 Dynamic Young's modulus determined after sintering by means of different methods and measuring systems: impulse excitation (RFDA) and ultrasonic testing (UKS-D, BP-700 Pro)

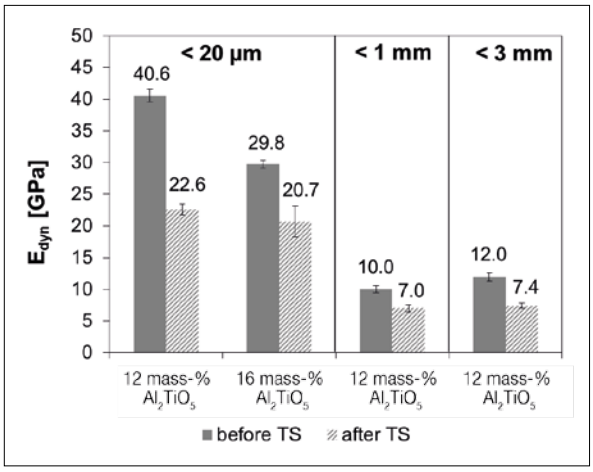

Fig. 6 Dynamic Young's modulus of the Al_2TiO_5-containing sintered bodies before and after quenching from 950 °C (Young's modulus was measured by ultrasonic testing using the UKS-D system)

12 mass-% of pre-synthesized aluminium titanate were influenced by the grain size distribution of the raw materials in the same order. However, the Al_2TiO_5-containing samples had significantly lower strengths and elastic moduli than those without Al_2TiO_5 despite lower porosities compared with the latter samples.

An increase of the added Al_2TiO_5 amount from 12–16 mass-% in the samples from the finest grain size fraction led to a further decrease in strength and Young's modulus. Microcracks within the aluminium titanate phase because of the thermal expansion anisotropy along the crystallographic axes (see section 1), microcracks caused by the mismatch between thermal expansion of spinel and aluminium titanate, and the enhanced grain growth can be assumed to contribute to this behaviour.

The microstructure of the samples with aluminium titanate was benefical for the thermal shock resistance of the ceramic. Non sample without Al_2TiO_5 but all tested Al_2TiO_5-containing specimens withstand quenching from 950 °C. The retained strengths and Young's moduli are shown in Fig. 4 and Fig. 6.

The addition of aluminium titanate had also a strong effect on the temperature dependence of the dynamic elastic modulus. Fig. 7a shows the change in Young's modulus during heating up to 1600 °C and subsequent cooling for a pure spinel sample from the raw material fraction <20 µm. The elastic modulus of this material exhibited a moderate, nearly linear decrease with increasing temperature, followed by a somewhat stronger decline in the upper temperature range. Such a behaviour is typical for many ceramic materials. The non-linear decrease at high temperatures is explained in the literature by "grain-boundary slip" [28]. Because densification of the pure spinel ceramic was not completed at the used sintering temperature of 1550 °C, sintering proceeded during the Young's modulus measurement. It is assumed that further is the explanation for the higher values of elastic modulus during cooling compared with the heating phase.

The Young's modulus of an Al_2TiO_5-containing sample from the finest raw material fraction as a function of temperature is shown in Fig. 7b. Starting from a significantly lower value at room temperature, the elastic modulus of this sample increased with increasing temperature until a plateau

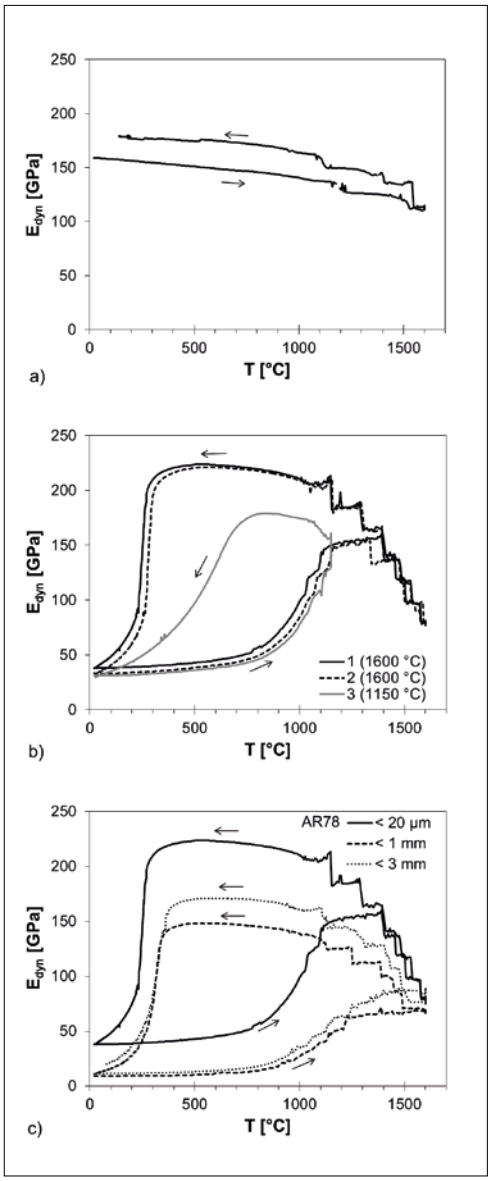

Fig. 7 Dynamic Young's modulus of sintered bodies as a function of temperature:
a) without Al_2TiO_5/from raw material <20 µm,
b) with 12 mass-% Al_2TiO_5/from raw material <20 µm; repeated measurements using the same test specimen (1st and 2nd measurement: T_{max} = 1600 °C, 3rd measurement: T_{max} = 1150 °C);
c) with 12 mass-% Al_2TiO_5; comparison of test specimens from raw materials with different maximum particle size: <20 µm, <1 mm, <3 mm
(Young's modulus was measured by impulse excitation using the RFDA apparatus)

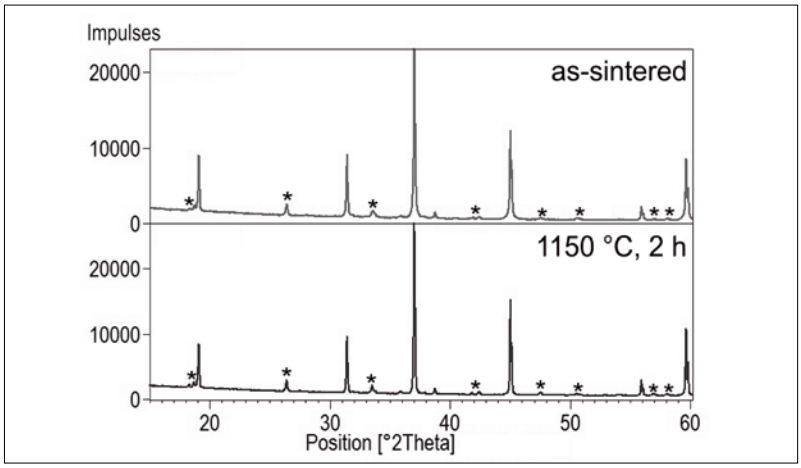

Fig. 8 X-ray diffractograms of MA spinel ceramic from raw material <20 µm with 12 mass-% Al_2TiO_5 after sintering and after subjecting a test specimen in the RFDA apparatus to a temperature of 1150 °C (see Fig. 7 b); *Al_2TiO_5

was reached at approximately 1130 °C. This behaviour can be attributed to microcrack closing during heating. Above a temperature of 1380 °C, a significant decrease in elastic modulus was observed. It could be assumed that a viscous phase is formed from the contained oxides including impurities. This would also be a possible explanation for the significant increase in Young's modulus during cooling. Decreasing the temperature below approximately 330 °C on cooling resulted in a sharp decline in elastic modulus because again microcracks are formed.

Despite a marginal shift, an identical curve was obtained when the measurement was repeated using the same sample (see Fig. 7b). In a third measurement, the sample was heated to a temperature in the decomposition range of aluminium titanate (1150 °C, 2 h dwell time) and afterwards analysed by XRD.

Again the Young's modulus increased during heating, but lower maximum values during cooling compared with the state after heating up to 1600 °C were obtained. Furthermore, the elastic modulus decreased on cooling already at higher temperatures and less steeply. As can be seen in Fig. 8, there was no indication of Al_2TiO_5 decomposition under the conditions of the Young's modulus measurement. Further experiments in a high-temperature furnace (see section 2) confirmed this result both for the sample from the finest raw materials fraction and for the samples from the coarse-grained Al_2TiO_5-containing powder mixtures. The curves of the latter samples started at lower room temperature elastic moduli but were very similar to those of the sample from the powder with particle sizes <20 µm, except for the behaviour in the upper temperature range (Fig. 7c). Because coarse grains reduce grain-boundary slip, the Young's modulus of the sintered bodies from the <1 mm and the <3 mm mixture did not decline in this range or exhibited only a slight decrease during the dwell time at 1600 °C, respectively.

4 Summary

The influence of aluminium titanate additions to Al_2O_3-rich magnesium aluminate spinel on the densification and microstructure evolution during sintering, on the strength and dynamic Young's modulus at room temperature, on the temperature dependence of the Young's modulus, and on the resistance to thermal shock has been shown.

Compared to pure MA spinel ceramic, the samples with Al_2TiO_5 exhibit higher densification and increased grain growth during sintering. Despite the lower porosity, the room temperature strengths and Young's moduli of the sintered bodies with aluminium titanate are significantly lower than those of the reference specimens without Al_2TiO_5. The Young's modulus of Al_2TiO_5-containing samples shows a pronounced hysteresis as a function of temperature.

By means of water quenching tests, it has been shown that the addition of aluminium titanate is an effective way to improve the thermal shock resistance of Al_2O_3-rich MA spinel refractories.

Acknowledgements

Financial support by the German Research Foundation (Deutsche Forschungsgemeinschaft, DFG) under Priority Program SPP 1418 Refractories – Initiative to Reduce Emissions – FIRE, is gratefully acknowledged.

The authors would like to thank Dr-Ing. Gert Schmidt for SEM investigations, Dipl.-Ing. Christian Ode for measuring the Young's modulus as a function of temperature, and Dipl.-Ing. Constantin Jahn for Young's modulus measurements by means of the UKS-D system.

References

[1] Buhr, A.: Refractories for steel secondary metallurgy. CN refractories **6** (1999) 19–30

[2] Buhr, A.; Laurich, J. O.: Synthetic alumina raw materials – key elements for innovative refractories. MPT Int. **3** (2000) 62–73

[3] Bradley, M.; Hutton, D.: An overview of refractory raw materials – Part 1: Alumina. The refractories Engineer (2011) May 20–23

[4] Aneziris, C. G.; et al.: Thermal shock performance of fine grained Al_2O_3 ceramics with TiO_2 and ZrO_2 additions for refractory applications. Adv. Engin. Mater. **12** (2010) 478–485

[5] Dudczig, S.; et al.: Nano- and micrometre additions of SiO_2, ZrO_2 and TiO_2 in fine grained alumina refractory ceramics for improved thermal shock performance. Ceram. Int. **38** (2011) 2011–2019

[6] Dudczig, S.; Aneziris, C. G.; Ballaschk, U.: Testing of thermal shock resistant fine grained alumina ceramics in a metal casting simulator. refractories WORLDFORUM **4** (2012) [1] 105–111

[7] Berek, H.; Aneziris, C. G.; Veres, D.: Interface reactions in fine-grained Al_2O_3 ceramics with TiO_2- and ZrO_2-additions for refractory applications as investigated by XCT and EBSD. refractories WORLDFORUM **4** (2012) [1] 85–90

[8] Aneziris, C. G.; Schärfl, W.; Ullrich, B.: Microstructure evaluation of Al_2O_3 ceramics with Mg–PSZ- and TiO_2-additions. J. Europ. Ceram. Soc. **27** (2007) 3191–3199

[9] Bayer, G.: Thermal expansion characteristics and stability of pseudobrookite-type compounds, M_3O_5. J. Less Common Metals **24** (1971) 129–138

[10] Cleveland, J. J.; Bradt, R. C.: Grain size/microcracking relations for pseudobrookite oxides. J. Amer. Ceram. Soc. **61** (1978) 478–481

[11] Ohya, Y.; Nakagawa, Z.; Hamano, K.: Grain boundary microcracking due to thermal expansion anisotropy in aluminum titanate ceramics. J. Amer. Ceram. Soc. **70** (1987) C185–C186

[12] Thomas, H. A. J.; Stevens, R.: Aluminum titanate – a literature review, Part II: Engineering properties and thermal stability. British Ceram. Trans. J. **88** (1989) 184–190

[13] Low, I. M.; Lawrence, D.; Smith, R. I.: Factors controlling the thermal stability of aluminum titanate ceramics in vacuum. J. Amer. Ceram. Soc. **88** (2005) 2957–2961

[14] Wohlfromm, H.; Moya, J. S.; Pena, P.: Effect of $ZrSiO_4$ and MgO additions on reaction sintering and properties of Al_2TiO_5-based materials. J. Mater. Sci. **25** (1990) 3753–3764

[15] Tilloca, G.: Thermal stabilization of aluminum titanate and properties of aluminum titanate solid solutions. J. Mater. Sci. **26** (1991) 2809–2814

[16] Freudenberg, B.; Mocellin, A.: Aluminum titanate formation by solid state reaction of fine Al_2O_3 and TiO_2 powders. J. Amer. Ceram. Soc. **70** (1987) 33–38

[17] Skiera, E.; et al.: Controlled crack propagation experiments with a novel alumina based refractory. Adv. Engin. Mater. **14** (2012) 248–254

[18] Hasselman, D. P. H.: Unified theory of thermal shock fracture initiation and crack propagation in brittle ceramics. J. Amer. Ceram. Soc. **52** (1969) 600–604

[19] Racher, R. P.; McConell, R. W.; Buhr, A.: Magnesium aluminate spinel raw materials for high performance refractories for steel ladles. Retrieved 6 December 2015 from www.almatis.com/media/3994/magnesium-aluminate-spinel-raw-materials-for-high-performance.pdf

[20] Moritz, K.; et al.: Thermal shock resistance of alumina and alumina-rich spinel refractories containing aluminum titanate. Proc. of the Unified Int. Technical Conf. on Refractories – UNITECR 2013 (Eds.: Goski, D.; Smith, J. D.), Hoboken, NJ, 2014, DOI: 10.1002/9781118837009.ch135

[21] Moritz, K.; et al.: Magnesium aluminate spinel ceramics containing aluminum titanate for refractory applications. J. Ceram. Sci. Technol. **5** (2014) 125–130

[22] Magnesium aluminate spinels. Product data, retrieved 6 December 2015 from www.almatis.com/media/58681/gp-rcp_004_magnesium_aluminate_spinel_0215.pdf

[23] Dinger, D. R.; Funk, J. E.: Particle packing V – computational methods applied to experimental distributions. Interceram **43** (1994) 87–89

[24 Buscaglia, V.; Nanni, P.: Decomposition of Al_2TiO_5 and $Al_{2(1-x)}Mg_xTi_{(1+x)}O_5$ ceramics. J. Amer. Ceram. Soc. **81** (1998) 2645–2653

[25] Low, I. M.; Oo, Z.: Reformation of phase composition in decomposed aluminum titanate. Mater. Chem. Phys. **111** (2008) 9–12

[26] Sathiyakumar, M.; Gnanam, F. D.: Influence of MnO and TiO_2 additives on density, microstructure and mechanical properties of Al_2O_3. Ceram. Int. **28** (2002) 195–200

[27] Sarkar, R.; Bannerjee, G.: Effect of TiO_2 on reaction sintered MgO–Al_2O_3 spinels. J. Europ. Ceram. Soc. **20** (2000) 2133–2141

[28] Wachtman, J. B. Jr.; Lam, D. G. Jr.: Young's modulus of various refractory materials as a function of temperature. J. Amer. Ceram. Soc. **42** (1959) 254–260